

# Strong Cation $\cdots\pi$ Interactions Promote the Capture of Metal Ions within Metal-Seamed Nanocapsule

Harshita Kumari,<sup>†</sup> Ping Jin,<sup>†</sup> Simon J. Teat,<sup>‡</sup> Charles L. Barnes,<sup>†</sup> Scott J. Dalgarno,<sup>§</sup> and Jerry L. Atwood<sup>\*,†</sup>

<sup>†</sup>Department of Chemistry, University of Missouri—Columbia, 601 South College Avenue, Columbia, Missouri 65211, United States

<sup>‡</sup>Beamline 11.3.1, Advanced Light Source, Lawrence Berkeley National Laboratory, 1 Cyclotron Road, MS6R2100, Berkeley, California 94720, United States

<sup>§</sup>Institute of Chemical Sciences, Heriot-Watt University, Riccarton, Edinburgh EH14 4AS, U.K.

## Supporting Information

**ABSTRACT:** Thallium ions are transported to the interior of gallium-seamed pyrogallol[4]arene nanocapsules. In comparison to the capture of Cs ions, the extent of which depends on the type and position of the anion employed in the cesium salt, the enhanced strength of Tl $\cdots\pi$  vs Cs $\cdots\pi$  interactions facilitates permanent entrapment of Tl<sup>+</sup> ions on the capsule interior. “Stitching-up” the capsule seam with a tertiary metal (Zn, Rb, or K) affords new trimetallic nanocapsules in solid state.

The synthesis of functional molecular containers is an area of intense current interest.<sup>1</sup> The design of complex architectures is a challenging goal, and introducing defects or tailoring their structures in order to modify chemical and physical properties is equally difficult.<sup>2</sup> For example, introducing defects on the basal planes of graphene or slicing carbon nanotubes induces chemical sensitivity or particular electronic properties.<sup>3</sup> Properties such as these are now being investigated in supramolecular synthons and in the resulting self-assembled architectures. Pyrogallol[4]arene macrocycles (Pgc $n$ , where  $n$  is the associated alkyl chain length) are vase-shaped cyclic oligomers of 1,2,3-trihydroxybenzene that have been shown to self-assemble into a range of dimeric and hexameric nanocapsules.<sup>2b–d,4</sup> The Pgc $n$  dimers and hexamers are composed of two and six macrocycles, with the prevailing assemblies seamed together with eight and 24 metal centers, respectively. In contrast, a nonsymmetric Pgc $n$  dimer can be generated by introducing a structural defect to the general Pgc $n$  bowl, by virtue of synthesizing a mixed resorcin[1]pyrogallol[3]arene macrocycle from resorcinol and pyrogallol.

This building block self-assembles into an asymmetric septa-metalated zinc dimer with an open channel for possible ion-transport studies.<sup>2b–d</sup> Inspired by such phenomena, we recently identified the gallium-seamed pyrogallol[4]arene hexameric nanocapsule (general formula [(Pgc $n$ )<sub>6</sub>Ga<sub>12</sub>(H<sub>2</sub>O)<sub>4</sub>]) as a suitable candidate for the introduction of structural defects/alterations.<sup>5</sup> As described below, unique structural differences observed for Pgc $n$ Ga-based nanoassemblies in solution vs the solid state renders them ideal for modification.<sup>5c</sup> Unlike the near-spherical hydrogen-bonded or transition metal (TM)-seamed Pgc $n$  nanocapsules, Ga-seamed assemblies adopt “rugby-ball”

shapes in the solid state.<sup>5d,e</sup> TM-seamed Pgc $n$  nanocapsules assemble as either dimers or hexamers with eight or 24 metal centers respectively;<sup>4,6</sup> these TM-seamed capsules have respective general formulae, [(Pgc $n$ )<sub>2</sub>TM<sub>8</sub>] and [(Pgc $n$ )<sub>6</sub>TM<sub>24</sub>], and can be accessed by different synthetic methods. Transition metal centers form the equatorial belt in the dimers, whereas they form M<sub>3</sub>O<sub>3</sub> triads along the faces of truncated octahedra in the hexamers.<sup>4,6,7</sup> In contrast, Ga has been shown to promote formation of only hexameric nanocapsules in the solid state; each Pgc $n$ /Ga hexamer contains 12 metal centers and four water gates that seam the six pyrogallol[4]arene units to form the general [(Pgc $n$ )<sub>6</sub>Ga<sub>12</sub>(H<sub>2</sub>O)<sub>4</sub>] nanocapsule.<sup>5d</sup> We previously showed that the addition of a secondary TM (Zn or Cu) to preformed Pgc<sub>4</sub>Ga nanocapsules adds 12 additional coordinating centers to the framework, causing a change from “rugby-ball” to near-spheroidal shape;<sup>5b</sup> the resulting nanocapsule thus has the general formula [(Pgc<sub>4</sub>)<sub>6</sub>Ga<sub>12</sub>Zn<sub>12</sub>]. Dramatic structural alterations are observed for Pgc<sub>4</sub>/Ga-based nanoassemblies in the solution phase. The [(Pgc<sub>4</sub>)<sub>6</sub>Ga<sub>12</sub>(H<sub>2</sub>O)<sub>4</sub>] nanocapsule is seen to change from “rugby-ball” to toroidal shape upon dissolution, and a similar change is also observed for [(Pgc<sub>4</sub>)<sub>6</sub>Ga<sub>12</sub>Zn<sub>12</sub>]<sup>5c</sup> (Figure 1). The solution-phase toroids were found to differ in metric dimensions. The Pgc<sub>4</sub>Ga toroid is ~17 Å in radius and ~7 Å in length, with Pgc<sub>4</sub> bowls oriented adjacent to one another with upper-rim hydroxyls exposed to the solvent.<sup>5c</sup> Radial and length dimensions of ~15 and ~13 Å are found for the Pgc<sub>4</sub>GaZn toroid, with Pgc<sub>4</sub> bowls oriented

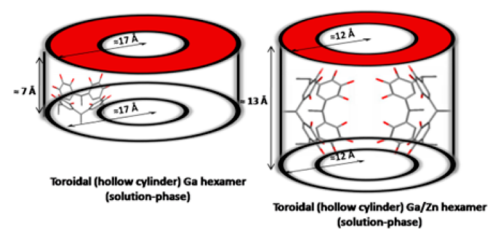


**Figure 1.** Schematic of toroidal Ga- and Ga/Zn-Pgc<sub>4</sub> nanoassemblies in acetone showing differences in the arrangement of bowls within the framework.

Received: October 19, 2014

Published: November 18, 2014

sideways and upper-rim hydroxyls forming the inner ring/core of the toroid.<sup>5c</sup>

These shape differences prompted us to investigate other properties such as ion transport across the water gates.<sup>5c</sup> Here we report our findings from the investigation of thallium ion transport across the structural water gates of  $[(\text{PgC4})_6\text{Ga}_{12}(\text{H}_2\text{O})_4]$ . Our particular interest in thallium arose from the fact that, in contrast to the  $\text{TM}^{+2}$  ions we have used to stitch up Ga-seamed hexamers, thallium has a +1 oxidation state and would thus exhibit markedly different behavior. Furthermore, we also wished to examine the level of incorporation of anions with respect to encapsulation, and explore their effect over the introduction of tertiary metal centers (Zn, K, and Rb). The latter goal was motivated by the potential to permanently and controllably trap guest species within fully metal-seamed hexamers.

As mentioned above, introduction of a secondary TM to a preformed  $\text{PgC}_4\text{Ga}$  nanocapsule led to replacement of the structural water gates.<sup>5a,b</sup> To investigate the fate of the  $\text{Tl(I)}$  ions, aqueous thallium nitrate (Supporting Information; SI) was added to an acetone suspension of preformed  $[(\text{PgC4})_6\text{Ga}_{12}(\text{H}_2\text{O})_4]$ . The resulting mixture was fully dissolved upon the addition of acetonitrile, and slow evaporation afforded single crystals that were suitable for diffraction studies. The crystals were in a triclinic cell, and structural solution was carried in the space group  $P\bar{1}$ . The asymmetric unit (ASU) consists of half of a nanocapsule containing encapsulated  $\text{Tl(I)}$  ions that form polyhaptoaromatic interactions with the  $\text{PgC4s}$  (Figure 2).

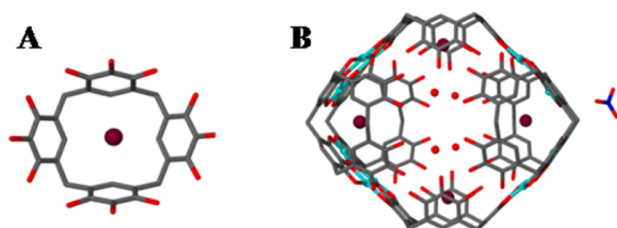


**Figure 2.** (A) Single pyrogallol[4]arene bowl showing the position of a thallium ion within the cavity. (B) Structure of the gallium-organic hexameric nanocapsules containing thallium ions on the interior (synthesized from thallium nitrate). Color code: C, gray; O, red; Ga, blue;  $\text{H}_2\text{O}$ , red spheres;  $\text{Tl}$ , purple; N, dark blue. H atoms and lower-rim  $\text{PgC}_n$  alkyl chains are omitted for clarity. Figures are not to scale.

Single-crystal XRD (scXRD) analyses indicate that the three crystallographically unique  $\text{Tl(I)}$  positions within the ASU have partial occupancies of 0.10, 0.10, and 0.5. A  $\text{Tl}$  ion is associated with each of the six bowls of pyrogallol[4]arene; however, the occupancy of  $\text{Tl}$  ion (refined via scXRD) is lower due to the disorder within the capsule interiors. The counterion, in this case nitrate, is located on the capsule exterior near the water gates, with hydrogen bonds present that are akin to those observed in the  $\text{PgC}_4\text{GaCCsNO}_3$  nanoassembly (Figure 1).<sup>8</sup> The reported structural rearrangement of  $[(\text{PgC4})_6\text{Ga}_{12}(\text{H}_2\text{O})_4]$  in solution<sup>5c</sup> suggests that  $\text{Tl(I)}$  encapsulation occurs via a similar mechanism; this would be via a transition from rugby-ball ( $[(\text{PgC4})_6\text{Ga}_{12}(\text{H}_2\text{O})_4]$ ) to toroid ( $[(\text{PgC4})_6\text{Ga}_{12}(\text{H}_2\text{O})_4]\text{CTl}$ ) to rugby-ball shape ( $[(\text{PgC4})_6\text{Ga}_{12}(\text{H}_2\text{O})_4]\text{CTl}$ ).

Once the entrapment of  $\text{Tl(I)}$  was established we investigated the effect of the addition of  $\text{Zn(II)}$  ions with a view to “stitching-up” this new assembly. The addition of an ethanolic solution of  $\text{Zn(II)}$  nitrate to an acetone solution of  $[(\text{PgC4})_6\text{Ga}_{12}(\text{H}_2\text{O})_4]\text{CTlNO}_3$  afforded single crystals that were suitable for

diffraction studies. Combined scXRD and elemental analysis confirms the formation of  $[(\text{PgC4})_6\text{Ga}_{11.5}\text{Zn}_{12.5}]\text{CTlNO}_3$  nanocapsule with  $\text{Tl(I)}$  ions disordered over six positions within pyrogallol[4]arene cavities (Figure 3; SI).

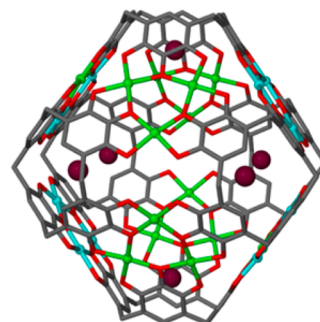


**Figure 3.** Structure of the  $\text{Ga/Zn-PgC}_n$  nanocapsule with trapped  $\text{Tl(I)}$  ions. Color code: C, gray; O, red; Ga, turquoise; Zn, green;  $\text{Tl}$ , purple spheres. H atoms and lower rim pyrogallol[4]arene alkyl chains are omitted for clarity.

Cation $\cdots\pi$  polyaromatic interactions have been observed in several calixarene-based systems.<sup>9</sup> For example, Cs complexes with calixarene in the absence of bulky p-substituents on the calix[4]arene through O-coordination and cation-polyhaptoaromatic interactions.<sup>9d</sup> Silver ions, however, complexes within both the cone and partial cone conformations of tetra-*O*-propylcalix[4]arene.<sup>9j</sup> Unlike the  $\text{Cs}^+$  ions by Thurey and co-workers, Beer and collaborators show  $\text{Tl}^+$  entrapment through the bulkier upper-rim substituents into the aromatic cavity of the calix[4]arene tubes.<sup>9k</sup>

The  $\text{Zn(II)}$  ions replace the structural water molecules, stitching the gates of the Ga-based hexamer, with concurrent structural transition from solid-state rugby-ball to solid-state spherical gallium–zinc hexamer. Elemental analysis reveals a total  $\text{Tl(I)}$  occupancy of 1.9 showing no ion escape from the framework. In previous studies, we found that encapsulated  $\text{Cs(I)}$  ions were expelled from the  $[(\text{PgC4})_6\text{Ga}_{12}(\text{H}_2\text{O})_4]$  framework upon the addition of  $\text{Zn(II)}$  ions.<sup>6</sup> In the present case  $\text{Tl(I)}$  ions are retained within the assembly, and this can clearly be attributed to the formation of stronger  $\text{Tl(I)}\cdots\pi$  interactions with the  $\text{PgC4s}$ . Factors, such as smaller ionic radius of  $\text{Tl(I)}$  (150 ppm) vs  $\text{Cs(I)}$  (167 ppm) and shorter cation $\cdots\pi$  (pyrogallol) interaction distances ( $\text{Tl(I)}\cdots\pi$  (centroid of pyrogallol), 3.38 to 3.60 Å, vs  $\text{Cs(I)}\cdots\pi$  (centroid of pyrogallol), 3.41 to 3.91 Å), contribute to stronger  $\text{Tl(I)}\cdots\pi$  interactions.

<sup>205</sup>Tl NMR studies were performed in order to further investigate these interactions, as well as differences in solid-versus solution-phase behavior. <sup>205</sup>Tl NMR of the acetone solution of preformed  $[(\text{PgC4})_6\text{Ga}_{12}(\text{H}_2\text{O})_4]\text{CTlNO}_3$  reveals two adjacent peaks at around –170 ppm, corresponding to bound  $\text{Tl(I)}$  ions (Figure 4). The absence of peaks at around 0 ppm indicates that both solid-state rugby-ball and solution-phase toroid  $[(\text{PgC4})_6\text{Ga}_{12}(\text{H}_2\text{O})_4]\text{CTlNO}_3$  nanoassemblies retain  $\text{Tl(I)}$  ions within the respective frameworks. Titration of  $\text{Zn(II)}$  ions does not produce peaks corresponding to free  $\text{Tl(I)}$  ions. Although this is the case, broadening of the peak at –170 ppm is observed, suggesting permanent entrapment of the  $\text{Tl(I)}$  ions.

To investigate anion effects over  $\text{Tl(I)}$  entrapment we synthesized  $[(\text{PgC4})_6\text{Ga}_{12}(\text{H}_2\text{O})_4]\text{CTl}_2(\text{SO}_4)$  by the addition of aqueous thallium sulfate to an acetone solution of  $[(\text{PgC4})_6\text{Ga}_{12}(\text{H}_2\text{O})_4]$ . The resulting mixture was dissolved in

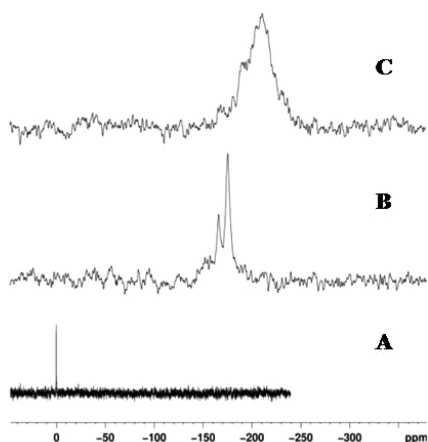


**Figure 4.**  $^{205}\text{Tl}$  NMR spectra or stackplot of (A) thallium nitrate (standard), (B)  $[(\text{PgC}_4)_6\text{Ga}_{12}\text{CTlNO}_3]$ , and (C)  $[(\text{PgC}_4)_6\text{Ga}_{12}\text{CTlNO}_3]$  upon titration with ethanolic zinc(II) nitrate indicating permanent entrapment of thallium ions.

acetonitrile, and slow evaporation afforded single crystals that were suitable for diffraction studies. Combined scXRD and elemental results confirm the entrapment of Tl(I) and sulfate ions within the Ga-based hexamer, with a total Tl(I) occupancy of 0.8 (SI). The occupancies for both the sulfate  $[(\text{PgC}_4)_6\text{Ga}_{12}(\text{H}_2\text{O})_4]\text{CTl}_2(\text{SO}_4)$  and nitrate  $[(\text{PgC}_4)_6\text{Ga}_{12}(\text{H}_2\text{O})_4]\text{CTl}(\text{NO}_3)$  complexes are similar. In contrast, the cesium sulfate complex led to a much higher  $\text{Cs}^+$  occupancy within the  $\text{PgC}_4\text{Ga}$  framework, emphasizing the effect of anion exclusively for  $\text{Cs}(\text{I})$  entrapment.<sup>8</sup>

In addition to the anion effects discussed above we also investigated the effect of stitching-up with a TM(II) ion (e.g., Zn(II)) vs K(I) or Rb(I). Crystals of Ga-PgC $n$  hexamers containing Tl(I) ions as either sulfate or nitrate complexes were dissolved in acetone and mixed with Rb(I) or K(I) nitrate water/acetonitrile solutions ( $v/v = 1:10$ ). Slow evaporation afforded single crystals suitable for diffraction studies in both cases. Structural analyses revealed the replacement of water gates by Rb and K ions and permanent entrapment of thallium ions within the  $[(\text{PgC}_4)_6\text{Ga}_{12}\text{Rb}_2/\text{K}_2]\text{CTl}(\text{NO}_3/\text{Ti}_2\text{SO}_4)$  nanocapsule for both sulfate and nitrate complexes (Figure 5).

The Rb/K ions are disordered over four positions within the nanocapsule and have total occupancies between 1 and 2. Importantly, the total occupancy of Tl(I) ions is not affected by the addition of sulfate or nitrate anionic complexes. Elemental analysis of both the nitrate and sulfate complexes formed upon Rb(I) addition reveals a total Tl(I)<sup>3</sup> occupancy of  $\sim 1.5$  per

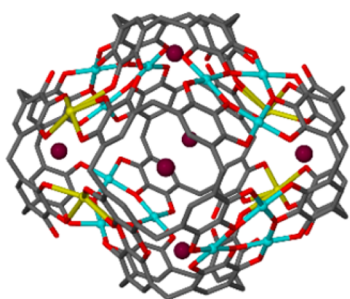


**Figure 5.** Structure of the Ga/Rb-PgC $n$  nanocapsule containing Tl(I) ions. Color code: C, gray; O, red; Ga, turquoise; Rb, yellow; Tl, purple. H atoms and lower-rim PgC $n$  alkyl chains are omitted for clarity.

nanocapsule. The addition of ethanolic Zn(II) nitrate to an acetone solution of either the nitrate or sulfate complex causes total replacement of Rb(I) ions within the gates, as confirmed by elemental analyses. This replacement occurs without displacement of the encapsulated guests; Tl(I) occupancy is found to be  $\sim 1.5$  per nanocapsule, further confirming the high affinity of the guest ions with the  $\text{PgC}_4$  aromatic rings.

In summary, ion-transport studies with  $\text{PgC}_4/\text{Ga}$ -based nanoassemblies show that Tl(I) ions can be transported to the capsule interior. The position of nitrate or sulfate anions with respect to the  $\text{PgC}_4\text{Ga}$  framework does not affect the entrapment or escape of Tl(I) ions from the capsule. The sulfate ions reside on the capsule interior, anchoring the Tl(I) ions, whereas nitrates are observed on the capsule exterior. The transport of Tl(I) occurs in solution phase and may be accompanied by structural alteration from solid-state rugby-ball to solution-phase toroid and back to solid-state rugby-ball framework, as suggested by XRD and small-angle neutron scattering (SANS) studies. Interestingly dissolution of both Tl(I) nitrate and sulfate complexes of  $[(\text{PgC}_4)_6\text{Ga}_{12}(\text{H}_2\text{O})_4]$  in acetone does not reveal any expulsion of guest ions, as evidenced by  $^{205}\text{Tl}$  NMR studies; this indicates the presence of strong  $\text{Tl}\cdots\pi$  interactions. Replacement of (a) water gates with Rb/K ions or (b) Rb/K gates with Zn(II) ions (for both sulfate and nitrate complexes) results in the formation of trimetallic nanoassemblies. Remarkably, unlike for Cs(I) ions, this replacement occurs without alteration of Tl(I) occupancy within the capsule framework, irrespective of the anion employed.<sup>8</sup> Furthermore, sulfate occupancy is also consistent. Future studies will focus on investigating this ion-transport phenomenon in tandem with SANS studies to fully elucidate structural alterations occurring in solution. Combined solid- and solution-phase studies will unravel new properties of metal-seamed organic nanoassemblies for further investigation and exploitation in host-guest chemistry.

## ■ ASSOCIATED CONTENT

### 📄 Supporting Information

Methods, NMR, and CIF files. This material is available free of charge via the Internet at <http://pubs.acs.org>.

## ■ AUTHOR INFORMATION

### ✉ Corresponding Author

atwoodj@missouri.edu

### 📝 Notes

The authors declare no competing financial interest.

## ■ ACKNOWLEDGMENTS

We thank the NSF (J.L.A.), NSF CHE-95-31247, and NIH 1S10RR11962-01 for financial support of this work. We also thank Dr. Wei G. Wycoff for NMR support and valuable discussions. The Advanced Light Source is supported by the Director, Office of Science, Office of Basic Energy Sciences, of the U.S. Department of Energy under Contract No. DE-AC02-05CH11231.

## ■ REFERENCES

- (1) Corbellini, F.; Knegtel, R. M. A.; Grootenhuys, P. D. J.; Crego-Calama, M.; Reinhoudt, D. N. *Chem.—Eur. J.* **2005**, *11*, 298.
- (2) Mansikkamäki, H.; Nissinen, M.; Rissanen, K. *CrystEngComm* **2005**, *7*, 519.
- (3) Moon, K.; Kaifer, A. E. *J. Am. Chem. Soc.* **2004**, *126*, 15016.
- (4) Jordan, J. H.; Gibb, B. C. *Chem. Soc. Rev.* **2014**, DOI: 10.1039/C4CS00191E.
- (5) Zarra, S.; Wood, D. M.; Roberts, D.



A.; Nitschke, J. R. *Chem. Soc. Rev.* **2014**, DOI: 10.1039/C4CS00165F.  
(f) Ma, D.; Hettiarachchi, G.; Nguyen, D.; Zhang, B.; Wittenberg, J. B.; Zavalij, P. Y.; Briken, V.; Isaacs, L. *Nat. Chem.* **2012**, *4*, 503. (g) Kim, D. S.; Sessler, J. L. *Chem. Soc. Rev.* **2014**, DOI: 10.1039/C4CS00157E.

(2) (a) Gianneschi, N. C.; Masar, M. S.; Mirkin, C. A. *Acc. Chem. Res.* **2005**, *38*, 825. (b) Fowler, D. A.; Rathnayake, A. S.; Kennedy, S. R.; Kumari, H.; Beavers, C. M.; Teat, S. J.; Atwood, J. L. *J. Am. Chem. Soc.* **2013**, *135*, 12184. (c) Bauer, F. *Appl. Phys. A: Mater. Sci. Process.* **2012**, *107*, 567. (d) Vedala, H.; Sorescu, D. C.; Kotchey, G. P.; Star, A. *Nano Lett.* **2011**, *11*, 2342.

(3) (a) Chen, X.; Dobson, J. F.; Raston, C. L. *Chem. Commun.* **2012**, 48, 3703. (b) Vimalanathan, K.; Chen, X.; Raston, C. L. *Chem. Commun.* **2014**, *50*, 11295.

(4) Dalgarno, S. J.; Power, N. P.; Atwood, J. L. *Coord. Chem. Rev.* **2008**, *252*, 825.

(5) (a) Jin, P.; Dalgarno, S. J.; Barnes, C.; Teat, S. J.; Atwood, J. L. *J. Am. Chem. Soc.* **2008**, *130*, 17262. (b) Jin, P.; Dalgarno, S. J.; Warren, J. E.; Teat, S. J.; Atwood, J. L. *Chem. Commun.* **2009**, 3348. (c) Kumari, H.; Kline, S. R.; Wycoff, W.; Paul, R. L.; Mossine, A. V.; Deakyne, C. A.; Atwood, J. L. *Angew. Chem.* **2012**, *51*, 5086. (d) McKinlay, R. M.; Thallapally, P. K.; Atwood, J. L. *Chem. Commun.* **2006**, 2956. (e) McKinlay, R. M.; Thallapally, P. K.; Cave, G. W. V.; Atwood, J. L. *Angew. Chem.* **2005**, *44*, 5733.

(6) Kumari, H.; Mossine, A. V.; Kline, S. R.; Dennis, C. L.; Fowler, D. A.; Teat, S. J.; Barnes, C. L.; Deakyne, C. A.; Atwood, J. L. *Angew. Chem.* **2012**, *51*, 1452.

(7) McKinlay, R. M.; Cave, G. W. V.; Atwood, J. L. *Proc. Natl. Acad. Sci. U.S.A.* **2005**, *102*, 5944.

(8) Kumari, H.; Jin, P.; Teat, S. J.; Barnes, C. L.; Dalgarno, S. J.; Atwood, J. L. *Angew. Chem.* **2014**, *53*, 13088.

(9) (a) Harrowfield, J. M.; Ogden, M. I.; Richmond, W. R.; White, A. H. *J. Chem. Soc., Chem. Commun.* **1991**, 1159. (b) Dalgarno, S. J.; Power, N. P.; Atwood, J. L. *Chem. Commun.* **2007**, 3447. (c) Dalgarno, S. J.; Szabo, T.; Siavosh-Haghighi, A.; Deakyne, C. A.; Adams, J. E.; Atwood, J. L. *Chem. Commun.* **2009**, 1339. (d) Thuéry, P.; Asfari, Z.; Vicens, J.; Lamare, V.; Dozol, J.-F. *Polyhedron* **2002**, *21*, 2497. (e) Hanna, T. A.; Liu, L.; Zakharov, L. N.; Rheingold, A. L.; Watson, W. H.; Gutsche, C. D. *Tetrahedron* **2002**, *58*, 9751. (f) Petrella, A. J.; Craig, D. C.; Lamb, R. N.; Raston, C. L.; Roberts, N. K. *Dalton Trans.* **2003**, 4590. (g) Harrowfield, J. M.; Ogden, M. I.; Richmond, W. R.; White, A. H. *J. Chem. Soc., Chem. Commun.* **1991**, 1159. (h) Ungaro, R.; Casnati, A.; Ugozzoli, F.; Pochini, A.; Dozol, J.-F.; Hill, C.; Rouquette, H. *Angew. Chem., Int. Ed.* **1994**, *33*, 1506. (i) Xu, W.; Puddephatt, R. J.; Muir, K. W.; Torabi, A. A. *Organometallics* **1994**, *13*, 3054. (j) Ikeda, A.; Tsuzuki, H.; Shinkai, S. *J. Chem. Soc., Perkin Trans. 2* **1994**, 2073. (k) Matthews, S. E.; Rees, N. H.; Felix, V.; Drew, M. G. B.; Beer, P. D. *Inorg. Chem.* **2003**, *42*, 729. (l) Couton, D.; Mocerino, M.; Rapley, C.; Kitamura, C.; Yoneda, A.; Ouchi, M. *Aust. J. Chem.* **1999**, *52*, 227. (m) Budka, J.; Lhoták, P.; Stibor, I.; Michlová, V.; Sykora, J.; Cisarová, I. *Tetrahedron Lett.* **2002**, *43*, 2857. (n) Harrowfield, J. K.; Ogden, M. I.; Richmond, W. R.; White, A. H. *J. Chem. Soc., Chem. Commun.* **1991**, 1159–1161.